Organic & Biomolecular Chemistry

This article is part of the

OBC 10th anniversary

themed issue

All articles in this issue will be gathered together online at

www.rsc.org/OBC10

Organic & Biomolecular Chemistry

Dynamic Article Links
View Online

Cite this: *Org. Biomol. Chem.*, 2012, **10**, 5769

www.rsc.org/obc

COMMUNICATION

Water-soluble, deep-red fluorescent squaraine rotaxanes†‡

Erin L. Cole,[a] Easwaran Arunkumar,[b] Shuzhang Xiao,[a] Bryan A. Smith[a] and Bradley D. Smith*[a]

Received 23rd October 2011, Accepted 22nd November 2011
DOI: 10.1039/c2ob06783h

Eight fluorescent squaraine rotaxanes with deep-red absorption/emission wavelengths were prepared and assessed for chemical stability and suitability as water-soluble, fluorescent tracers. The most stable squaraine rotaxanes have four large stopper groups attached to the ends of the encapsulated squaraine, and two members of this structural class have promise as highly fluorescent tracers with rapid renal clearance and very low tissue uptake in living mice.

Squaraines are intensely colored and highly fluorescent dyes with deep-red emission wavelengths.[1] They have been studied for many photonic applications but their utility for biological imaging is limited by their susceptibility to chemical attack by strong nucleophiles and hydrolytic decomposition in aqueous solution.[2] In 2005, we reported a method to permanently encapsulate squaraine dyes inside macrocyclic tetralactams and create squaraine rotaxanes.[3] This encapsulation process greatly enhances dye stability and also circumvents the problem of fluorescence quenching upon self-aggregation.[4] We have subsequently shown that squaraine rotaxanes can be employed as targeted fluorescent molecular probes for cell microscopy and whole-body imaging of disease models in small living animals.[5] To date, most of the squaraine rotaxane probes have been lipophilic or partially soluble in water or related aqueous buffers. However, there is a need for squaraine rotaxanes that are highly water-soluble. Applications for these types of compounds would range from targeted bioconjugates for molecular imaging to non-targeted fluorescent tracers for various biomedical and analytical methods.[6,7]

The chemical conversion of hydrophobic fluorescent dyes into water-soluble, non-aggregating compounds is a non-trivial task, especially for near-infrared dyes because they have relatively reactive chromophores and large hydrophobic surfaces.[8] The synthetic process has to introduce water-solubilizing groups into the dye structure in a way that does not degrade the photophysical performance. In the case of squaraine rotaxanes, there is the additional design constraint of ensuring that the protective macrocycle remains tightly held over the reactive squaraine dye.[9] Here, we describe the synthesis and deep-red absorption/emission properties of water-soluble squaraine rotaxanes, **1–8** (Scheme 1), and we assess chemical stabilities in conditions that mimic physiological environments. We find that the size of the four stopper groups appended to the ends of the encapsulated squaraine dye is a crucial factor in determining long-term, chemical stability in physiological solution. The most stable squaraine rotaxanes have four large stopper groups and we have identified two members of this structural class as non-targeted, fluorescent tracers with bright, deep-red emissions and high suitability for biological imaging.

The syntheses of squaraine rotaxanes **1–8** are described in the Electronic Supplementary Information (ESI).‡ The rotaxanes were prepared by conducting Leigh-type clipping reactions that permanently trapped an organic soluble squaraine dye inside a tetralactam macrocycle that was composed of two phenylene side walls and two pyridine 2,6-carboxamide bridging units.[4a] In most cases, copper catalyzed azide-alkyne cycloaddition chemistry was used to attach appropriately protected polar groups to the ends of the encapsulated squaraine dye, and subsequent deprotection provided **1–8** with high water-solubility (each compound readily dissolved to form a 20 μM aqueous solution). Listed in Table 1 are the absorption/emission properties in water. Each sample exhibited the expected narrow deep-red absorption band in the region of 651–654 nm, fluorescence emission with an approximate 20 nm Stokes shift, and fluorescence quantum yields of 0.16–0.24.§ Chemical and photochemical stability was measured by monitoring the squaraine absorbance maxima in pure water and 10% FBS (fetal bovine serum). The two graphs

Table 1 Absorption/emission maxima in water

Compound	λ_{abs} (nm)	log ε	λ_{em} (nm)	Φ_f [a]
1	651	5.6	672	0.22
2	655	5.1	677	0.16
3[b]	653	5.1	675	0.20
4	654	5.1	675	0.22
5	654	5.1	675	0.21
6	653	5.3	672	0.24
7	652	5.3	673	0.23
8	653	5.2	674	0.23

[a] Fluorescence quantum yields (error limit ± 5%) were determined using 4,4′-[bis(*N*,*N*-dimethylamino)phenyl]squaraine dye as the standard (Φ_f = 0.70 in $CHCl_3$). [b] Reported previously in ref. 5a.

[a]*Department of Chemistry and Biochemistry, University of Notre Dame, Notre Dame, IN, 46556, USA. E-mail: smith.115@nd.edu*
[b]*Molecular Targeting Technologies Incorporated, 833 Lincoln Ave., Unit 9, West Chester, PA, 19380, USA*

† This article is part of the *Organic & Biomolecular Chemistry* 10th Anniversary issue.

‡ Electronic supplementary information (ESI) available: Synthetic methods, spectral data, photophysical measurements, and protocol for approved animal study. See DOI: 10.1039/c2ob06783h

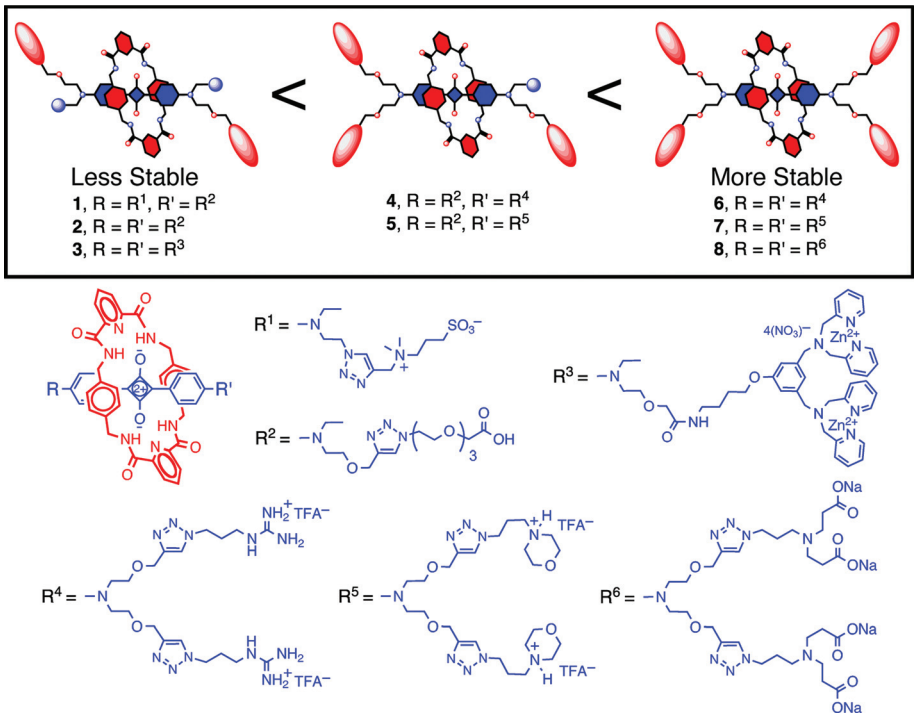

Scheme 1 Structures of squaraine rotaxanes and the trend for aqueous stability.

in Fig. 1 show stability curves for samples that were exposed to laboratory lights (control samples stored in the dark gave the same results). The data are consistent with the general stability trend that is summarized in Scheme 1. That is, squaraine rotaxane stability in water is related to the total number of large stopper groups (*i.e.*, groups larger than *N*-ethyl) attached to the two terminal squaraine nitrogen atoms, in the approximate order of four > three > two. The most stable squaraine rotaxanes in water are **6–8**, each with four large stopper groups, although **6** undergoes some moderate decomposition in serum. The hydrolytic susceptibility of rotaxanes **1–5**, with only two or three large stopper groups, suggests that the surrounding macrocycle has enough translational mobility in aqueous solution to transiently expose the reactive core of the encapsulated squaraine. This macrocycle mobility is limited by the steric hindrance imposed by the four large stopper groups in **7** and **8**.¶ The excellent photochemical stabilities of **7** and **8** were confirmed by irradiating aerated aqueous samples with a 45 W fluorescent bulb at a distance of 30 cm for two hours and observing absorption losses of only 4% and 1%, respectively. The high resistance to photobleaching is not surprising since squaraine rotaxanes are weak oxygen photosensitizers and relatively unreactive with singlet oxygen.[4a] It is also worth noting that squaraine rotaxanes are typically not phototoxic; for example, previous studies of bacterial cells that were stained with squaraine rotaxane **3** showed that the cells remained viable after extended irradiation periods.[5]

The hydrolytic instabilities of **1–6** indicate that these structures are not well-suited for further development into high stability, fluorescent bioimaging probes. However, the excellent chemical and photochemical stabilities of squaraine rotaxanes **7** and **8** prompted us to assess their potential as water-soluble, deep-red fluorescent tracers. Fluorescent dyes that emit light in the wavelength window of 650–900 nm are known to possess bioimaging performance advantages such as maximum penetration of the light through skin and tissue and inherently high contrast due to minimized background autofluorescence.[10] Nonetheless, deep-red and near-infrared dyes are rarely employed as hydrophilic fluorescent tracers, in part, because they self-quench in water at concentrations above a few micromolar, which prohibits quantitative fluorescence measurements.[6,7,11] This drawback seems especially prevalent with cyanine dyes, the most common class of near-infrared dyes.[12] Therefore, it is notable that squaraine rotaxanes **7** and **8** exhibit excellent Beer–Lambert absorption/emission behavior up to 14 μM, the highest concentration tested (Fig. 2). As expected, the emission plots are slightly curved at higher concentrations because the absorption/emission bands are partially overlapping which produces an inner filter effect.[13] Additional absorption/emission studies of **7** and **8** showed that the brightness (molar absorptivity × fluorescence quantum yield) is unchanged over the pH range of 6 to 10. Finally, equilibrium dialysis experiments with mixtures of **7** or **8** with bovine serum albumin indicated weak dye/albumin protein association (see ESI‡).

The low affinity of squaraine rotaxanes **7** or **8** for albumin protein suggested that they may be useful as non-targeted, control tracers in our ongoing project to develop targeted squaraine rotaxane probes for *in vivo* molecular imaging. Therefore, a mouse biodistribution study was conducted to determine the extent of non-selective tissue and organ retention of **7** and **8**. All animal procedures were approved by the University of Notre Dame Institutional Animal Care and Use Committee. As a benchmark, we also included the near-infrared fluorophore, Indocyanine Green (**ICG**), a clinically approved dye that is commonly employed as a non-targeted tracer for *in vivo* imaging studies.[14] Three cohorts of mice were dosed intravenously with an aqueous solution of one of the three dyes (40 pmol g^{-1}) and each animal was sacrificed two hours later. The skin overlaying

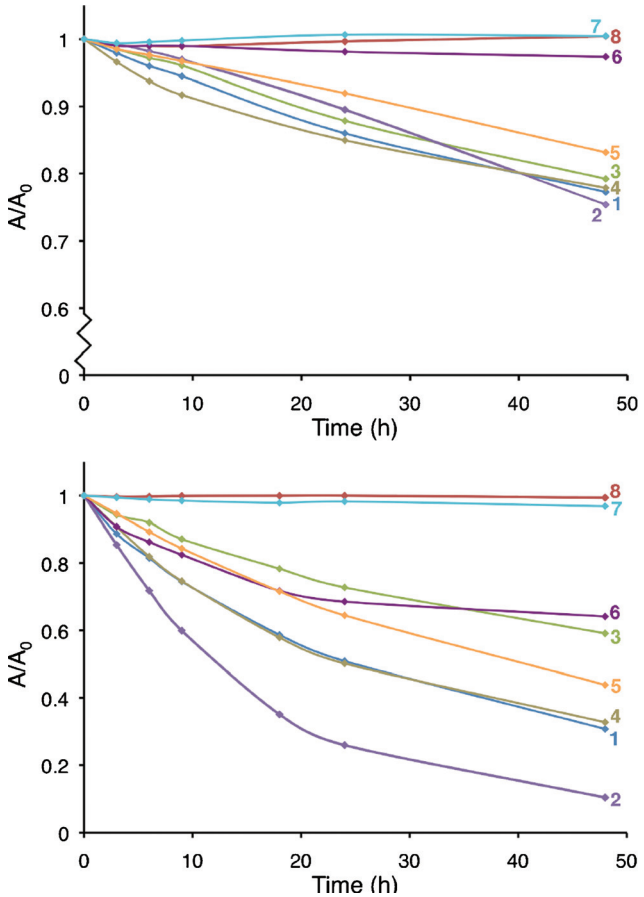

Fig. 1 Change in squaraine rotaxane absorption (5 μM) at wavelength maxima in pure water (top) and 10% FBS in water (bottom), $T = 25°$ C. Samples were exposed to laboratory lights throughout the experiment. Note that the fluorescence spectra of **7** and **8** were also unchanged over time indicating no longitudinal change in fluorescence quantum yield.

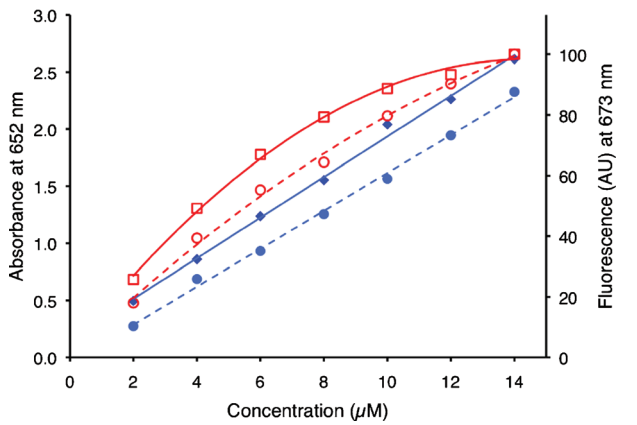

Fig. 2 Absorption and emission intensities at different concentrations in phosphate buffered saline (sodium phosphate 10 mM, NaCl 150 mM, pH 7.4): (a) **7** em (red open squares); (b) **8** em (red open circles); (c) **7** abs (blue filled diamonds); (d) **8** abs (blue filled circles). Linear fits of the two absorption plots have R^2 values >0.99; the curved lines for the fluorescence plots are simply to guide the eye.

the abdominopelvic cavity was resected and optical images were taken of the intact organs using an *in vivo* imaging station that was equipped with appropriate illumination/emission filter sets and a sensitive CCD camera. Shown in Fig. 3 are representative brightfield image and fluorescence intensity maps for mice treated with each dye. The fluorescence images indicate relative biodistribution of the tracers, and in the case of **7** and **8** the tracers are primarily in the urine remaining in the bladder, with very little uptake by the other organs. In comparison, there was very little **ICG** in the bladder but a very intense signal in the intestines. This was expected since **ICG** is known to be cleared from the bloodstream by the biliary system and subsequently excreted into the intestines.[14]

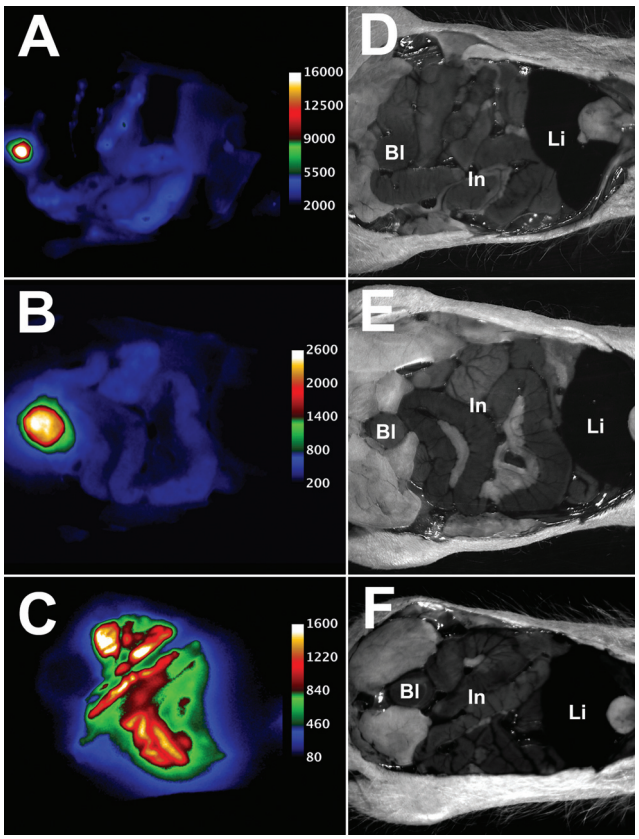

Fig. 3 Fluorescence intensity maps (ex: 630 ± 10 nm, em: 700 ± 20 nm) and brightfield images (50 mm field of view) of the exposed abdominopelvic cavities of representative mice treated intravenously with 40 pmol g^{-1} of **7** (A,D), **8** (B,E), or **ICG** (C,F) and sacrificed at two hours post-injection of fluorophore. Abbreviations: bladder (Bl), intestines (In), liver (Li). Note that the physical area of the bladder signal in A is smaller than B but the pixel intensity is higher. The fluorescence intensity scale for each image is in arbitrary units.

The biodistributions of **7** and **8** were further compared by *ex vivo* fluorescence imaging of the excised organs. Region of interest analysis of the pixel intensity maps in Fig. 4 allowed calculation of mean pixel intensity for each excised tissue. The squaraine fluorophores in **7** and **8** have essentially the same deep-red absorption/emission wavelengths and the same brightness, so the mean pixel intensity values reflect relative levels of dye in each tissue sample. The sum of mean pixel intensity values for **7** in all the excised tissues is 9.3 times greater than the analogous value for **8**. We conclude that non-selective retention of water-soluble, squaraine rotaxane **7** by the tissues and organs of living animals is quite low, and that the tissue retention of

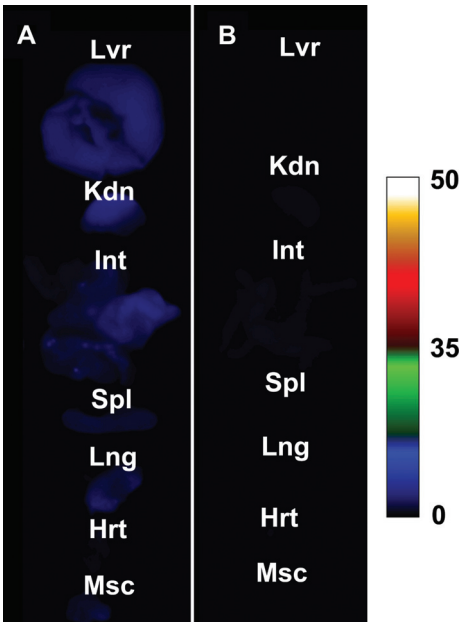

Fig. 4 Comparative fluorescence intensity maps (ex: 630 ± 10 nm, em: 700 ± 20 nm) of excised tissue and organs of mice treated intravenously with 40 pmol g^{-1} of **7** (A) or **8** (B) and sacrificed at two hours post-injection of fluorophore. Abbreviations: liver (Lvr), kidney (Kdn), intenstines (Int), spleen (Spl), lung (Lng), heart (Hrt), muscle (Msc). Fluorescence intensity scale in arbitrary units.

tracer **8** is even lower. The rapid excretion of **8** through the kidneys is especially notable, and quite obvious to the naked eye since the mouse urine turns blue within a few minutes after intravenous dosage. Recently, other research groups have observed high renal clearance of dyes and small nanoparticles (hydrodynamic radius ≤ 5 nm) with structures having a mixed and geometrically balanced distribution of positive and negative charges.[6,15] The structure of squaraine rotaxane **8** seems to agree with this trend but there is one significant difference. Choi and coworkers reported that the dyes must have a mixture of permanent charges such as quaternary ammoniums and sulfonates, and not weakly charged groups like carboxylates and protonated ammoniums.[6] We believe that the dendritic and polyionic structure of **8** (primarily a mixture of eight anionic carboxylates and four cationic ammoniums at physiological pH, see Scheme 2), is an additional structural factor that promotes rapid renal clearance because it favors extensive hydration of the molecular periphery, screening of electrostatic charge, and avoidance of biological surfaces.

In summary, the long-term hydrolytic instability of water-soluble squaraine rotaxanes **1–5** is attributed to the relatively small steric size of the *N*-ethyl stopper group that is attached to one or both ends of the encapsulated squaraine (Scheme 1). The most stable squaraine rotaxanes in water are **6–8**, each with four large stopper groups, although **6** undergoes some moderate decomposition in serum. As deep-red fluorescent tracers, squaraine rotaxane **7**, and especially **8**, exhibit an attractive collection of properties including very high chemical and photochemical stability, low phototoxicity, resistance to self-quenching, high and pH-independent brightness, and negligible uptake by mammalian tissue. In the near future, we will publish reports showing the utility of **8** as a non-targeted, fluorescent tracer for whole-body molecular imaging studies of living animals. We expect that deep-red fluorescent tracers **7** and **8** will be broadly useful in other types of biomedical, analytical, and biotechnology applications.[7]

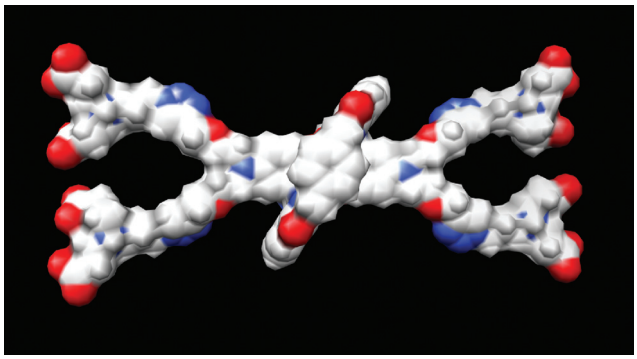

Scheme 2 Molecular model of squaraine rotaxane **8** at physiological pH showing electrostatic surface with positive centers colored blue and negative centers red. The longest diagonal length of the extended molecule is ~4.6 nm.

Acknowledgements

This work that was supported by NIH grants R43-EB009266 and T32GM075762. The mouse imaging protocol was approved by the Notre Dame Institutional Committee for Animal Care and the molecular model in Scheme 2 was created by the Notre Dame Center for Research Computing.

Notes and references

§ The ESI‡ contains photophysical properties for rotaxanes **1–8** in phosphate buffered saline (PBS, sodium phosphate 10 mM, NaCl 150 mM, pH 7.4) and 10% FBS (fetal bovine serum), and they are nearly identical to the PBS data Table 1. Also provided in the ESI‡ are photophysical properties of the precursor squaraine dyes, and inspection of this data shows that encapsulation inside the macrocyclic tetralactam induces a 7–10 nm red-shift in squaraine absorption/emission maxima and a slight increase in fluorescence quantum yield.
¶ Even at 37 °C, compound **8** exhibited extremely high stability in 10% FBS.

1 (*a*) K.-Y. Law, *Chem. Rev.*, 1993, **93**, 449–486; (*b*) K.-Y. Law, in *Organic Photochemistry*, ed. V. Ramamurthy and K. S. Schanze, Marcel Dekker, New York, 1997, p 519; (*c*) S. Das, K. G. Thomas and M. V. George, in *Organic Photochemistry*, ed. V. Ramamurthy and K. S. Schanze, Marcel Dekker, New York, 1997, p 467.
2 (*a*) J. Ros-Lis, B. Garcia, D. Jimenez, R. Martinez-Manez, F. Sancenon, J. Soto, F. Gonzalvo and M. Valldecabres, *J. Am. Chem. Soc.*, 2004, **126**, 4064–4065; (*b*) S. Sreejith, K. P. Divya and A. Ajayaghosh, *Angew. Chem., Int. Ed.*, 2008, **47**, 7883–7887.
3 E. Arunkumar, C. C. Forbes, B. C. Noll and B. D. Smith, *J. Am. Chem. Soc.*, 2005, **127**, 3288–3289.
4 (*a*) J. J. Gassensmith, J. M. Baumes and B. D. Smith, *Chem. Commun.*, 2009, 6329–6338; (*b*) M. T. Stone and H. L. Anderson, *Chem. Commun.*, 2007, 2387–2389.
5 (*a*) J. R. Johnson, N. Fu, E. Arunkumar, W. M. Leevy, S. T. Gammon, D. Piwnica-Worms and B. D. Smith, *Angew. Chem., Int. Ed.*, 2007, **46**, 5528–5531; (*b*) A. G. White, N. Fu, W. M. Leevy, J.-J. Lee, M. A. Blasco and B. D. Smith, *Bioconjugate Chem.*, 2010, **21**, 1297–1304.
6 H. S. Choi, K. Nasr, S. Alyabyev, D. Feith, J. H. Lee, S. H. Kim, Y. Ashitate, H. Hyun, G. Patonay, L. Strekowski, M. Henary and J. V. Frangioni, *Angew. Chem., Int. Ed.*, 2011, **50**, 6258–6263.
7 For recent books and articles on fluorescent dyes as sensors and tracers, see: (*a*) A. P. Demchenko, in *Introduction to Fluorescence Sensing*,

Springer, New York, 2009; (*b*) S. Heckl, *Curr. Med. Chem.*, 2007, **14**, 1713–1728; (*c*) A. K. Chen, Z. Cheng, M. A. Behlke and A. Tsourkas, *Anal. Chem.*, 2008, **80**, 7437–7444; (*d*) R. Rajagopalan, W. L. Neumann, A. R. Poreddy, R. M. Fitch, J. N. Freskos, B. Asmelash, K. R. Gaston, K. P. Galen, J.-J. Shieh and R. B. Dorshow, *J. Med. Chem.*, 2011, **54**, 5048–5058; (*e*) A. Vercelli, M. Repici, D. Garbossa and A. Grimaldi, *Brain Res. Bull.*, 2000, **51**, 11–28; (*f*) J. M. Baumes, J. J. Gassensmith, J. Giblin, J.-J. Lee, A. G. White, W. J. Culligan, W. M. Leevy, M. Kuno and B. D. Smith, *Nat. Chem.*, 2010, **2**, 1025–1030.

8 For recent articles on water-soluble red and near-infrared fluorescent dyes, see: (*a*) S. K. Yang, X. Shi, S. Park, S. Doganay, T. Ha and S. C. Zimmerman, *J. Am. Chem. Soc.*, 2011, **133**, 9964–9967; (*b*) F. Shao, H. Yuan, L. Josephson, R. Weissleder and S. A. Hilderbrand, *Dyes Pigm.*, 2011, **90**, 119–122; (*c*) C. Ornelas, R. Lodescar, A. Durandin, J. W. Canary, R. Pennell, L. F. Liebes and M. Weck, *Chem.–Eur. J.*, 2011, **17**, 3619–3629; (*d*) J. Pauli, M. Grabolle, R. Brehm, M. Spieles, F. M. Hamann, M. Wenzel, I. Hilger and U. Resch-Genger, *Bioconjugate Chem.*, 2011, **22**, 1298–1308; (*e*) H. H. Gorris, S. M. Saleh, D. B. M. Groegel, S. Ernst, K. Reiner, H. Mustroph and O. S. Wolfbeis, *Bioconjugate Chem.*, 2011, **22**, 1433–1437; (*f*) S. L. Niu, C. Massif, G Ulrich, R. Ziessel, P.-Y. Renard and A. Romieu, *Org. Biomol. Chem.*, 2011, **9**, 66–69; (*g*) T. Bura and R. Ziessel, *Org. Lett.*, 2011, **13**, 3072–3075; (*h*) M. Tasior and D. F. O'Shea, *Bioconjugate Chem.*, 2010, **21**, 1130–1133; (*i*) J.-A. Richard, M. Massonneau, P.-Y. Renard and A. Romieu, *Org. Lett.*, 2008, **10**, 4175–4178; (*j*) Y. Yang, M. Lowry, X. Xu, J. O. Escobedo, M. Sibrian-Vazquez, L. Wong, C. M. Schowalter, T. J. Jensen, F. R. Fronczek, I. M. Warner and R. M. Strongin, *Proc. Natl. Acad. Sci. U. S. A.*, 2008, **105**, 8829–8834; (*k*) K. Kolmakov, V. N. Belov, J. Bierwagen, C. Ringemann, V. Muller, C. Eggeling and S. W. Hell, *Chem.–Eur. J.*, 2010, **16**, 158–166; (*l*) Y. N. Teo, J. N. Wilson and E. T. Kool, *J. Am. Chem. Soc.*, 2009, **131**, 3923–3933; (*m*) V. Fernández-Moreira, F. L. Thorp-Greenwood and M. P. Coogan, *Chem. Commun.*, 2010, **46**, 186–202; (*n*) L. Cosgrave, M. Devocelle, R. J. Forster and T. E. Keyes, *Chem. Commun.*, 2010, **46**, 103–105; (*o*) J.-S. Lee, Y. K. Kim, M. Vendrell and Y.-T. Chang, *Mol. BioSyst.*, 2009, **5**, 411–421; (*p*) M. V. Reddington, *Bioconjugate Chem.*, 2007, **18**, 2178–2190; (*q*) K. Umezawa, D. Citterio and K. Suzuki, *Anal. Sci.*, 2008, **24**, 213–217; (*r*) K. Kiyose, S. Aizawa, E. Sasaki, H. Kojima, K. Hanaoka, T. Terai, Y. Urano and T. Nagano, *Chem.–Eur. J.*, 2009, **15**, 9191–9200; (*s*) J. Jose, Y. Ueno and K. Burgess, *Chem.–Eur. J.*, 2009, **15**, 418–423; (*t*) A. Romieu, D. Brossard, M. Hamon, H. Outaabout, C. Portal and P.-Y. Renard, *Bioconjugate Chem.*, 2008, **19**, 279–289.

9 (*a*) N. Fu, J. J. Gassensmith and B. D. Smith, *Supramol. Chem.*, 2009, **21**, 118–124; (*b*) E. Arunkumar, N. Fu and B. D. Smith, *Chem.–Eur. J.*, 2006, **12**, 4684–4690.

10 K. Licha, *Top. Curr. Chem.*, 2002, **222**, 1–29.

11 J. O. Escobedo, O. Rusin, S. Lim and R. M. Strongin, *Curr. Opin. Chem. Biol.*, 2010, **14**, 64–70.

12 (*a*) A. Mishra, R. K. Behera, P. K. Behera, B. K. Mishra and G. B. Behera, *Chem. Rev.*, 2000, **100**, 1973–2011; (*b*) M. Levitus and S. Ranjit, *Q. Rev. Biophys.*, 2011, **44**, 123–151.

13 N. J. Turro, V. Ramamurthy and J. C. Scaiano, in *Principles of Molecular Photochemistry: An Introduction*, University Science, Sausalito, 2009, Ch. 7.

14 (*a*) T. Desmettre, J. M. Devoisselle and S. Mordon, *Surv. Ophthalmol.*, 2000, **45**, 15–27; (*b*) B. H. Yuan, N.-G. Chen and Q. Zhu, *J. Biomed. Opt.*, 2004, **9**, 497–503.

15 (*a*) J. Park, J. Nam, N. Won, H. Jin, S. Jung, S. Jung, S.-H. Cho and S. Kim, *Adv. Funct. Mater.*, 2011, **21**, 1558–1566; (*b*) H. S. Choi, Y. Ashitate, J. H. Lee, S. H. Kim, A. Matsui, N. Insin, M. G. Bawendi, M. Semmler-Behnke, J. V. Frangioni and A. Tsuda, *Nat. Biotechnol.*, 2010, **28**, 1300–1303; (*c*) H. Kobayashi, N. Le, I.-S. Kim, M.-K. Kim, J.-E. Pie, D. Drumm, D. S. Paik, T. A. Waldmann, C. H. Paik and J. A. Carrasquillo, *Cancer Res.*, 1999, **59**, 422–430.